On the shape of the cross-ratio function in bivariate survival models induced by truncated and folded normal frailty distributions

Steffen Unkel

Department of Medical Statistics, University Medical Center Göttingen, Humboldtallee 32, 37073 Göttingen, Germany

May 1, 2016

Abstract

In shared frailty models for bivariate survival data the frailty is identifiable through the cross-ratio function (CRF), which provides a convenient measure of association for correlated survival variables. The CRF may be used to compare patterns of dependence across models and data sets. We explore the shape of the CRF for the families of one-sided truncated normal and folded normal frailty distributions.

Keywords: Cross-ratio function, Frailty, Heterogeneity, Student-t distributions, Survival data, Truncation

---

1. Setting the scene

Consider bivariate time-to-event data and let T_j $(j = 1, 2)$ be the two failure times of interest with marginal survivor functions $S_j(t_j)$ and joint survival function $S(t_1, t_2)$. The hazard rate at time t for an individual with a random effect $Z \geq 0$ with density $f(Z)$ having finite mean and finite variance, denoted $h_j(t, Z)$, is assumed to be of the form

$$h_j(t, Z) = Z \cdot h_{0j}(t) \ , \tag{1}$$

for $j = 1, 2$, where the baseline hazards $h_{0j}(t)$ are independent of Z and describe the time effect. The random variation in Z induces association between

---

Email address: `steffen.unkel@med.uni-goettingen.de` (Steffen Unkel)

the two failure times T_1 and T_2; T_1 and T_2 are conditionally independent given $Z = z$. The individual latent effects capture the unobserved heterogeneity between the individuals and may be viewed as individual frailties, yielding shared frailty models for the hazard rates (Duchateau and Janssen, 2008; Hougaard, 2000; Wienke, 2011).

A convenient local association measure for bivariate survival data is the cross-ratio function (CRF) (Clayton, 1978), which at (t_1, t_2) is defined as

$$\theta^*(t_1, t_2) = \frac{S(t_1, t_2)\, \mathrm{D}_1\mathrm{D}_2 S(t_1, t_2)}{\mathrm{D}_1 S(t_1, t_2)\, \mathrm{D}_2 S(t_1, t_2)} \ , \tag{2}$$

where D_j denotes the derivative operator $\partial/\partial t_j$. The definition (2) lacks an obvious interpretation. However, since $\mathrm{D}_1\mathrm{D}_2 S(t_1, t_2)/\mathrm{D}_2 S(t_1, t_2) = f(t_1|T_2 = t_2)/S(t_1|T_2 = t_2)$ and $\mathrm{D}_1 S(t_1, t_2)/S(t_1, t_2) = f(t_1|T_2 > t_2)/S(t_1|T_2 > t_2)$, where $f(t)$ denotes the probability density function (pdf) of a random variable T, (2) is related to the hazard of events. It is the ratio of the hazard of T_1 given T_2 has taken place at time t_2 over the hazard of T_1 given T_2 has not yet taken place at t_2 (Oakes, 1989). Furthermore, Anderson et al. (1992) showed that for $\epsilon > 0$:

$$\lim_{\epsilon \to 0} \mathrm{OR}(t_1, t_2; \epsilon) \doteq \theta^*(t_1, t_2) \ ,$$

where the odds ratio $\mathrm{OR}(t_1, t_2; \epsilon)$ is defined as

$$\mathrm{OR}(t_1, t_2; \epsilon) = \frac{\mathrm{odds}(t_1 < T_1 \le t_1 + \epsilon \mid T_1 > t_1, t_2 < T_2 \le t_2 + \epsilon)}{\mathrm{odds}(t_1 < T_1 \le t_1 + \epsilon \mid T_1 > t_1, T_2 > t_2 + \epsilon)} \ .$$

Thus, the CRF has a local odds ratio interpretation as it approximates $\mathrm{OR}(t_1, t_2; \epsilon)$ in an instant past (t_1, t_2) (see also Clayton and Cuzick (1985)). The CRF can also be interpreted as a local version of Kendall's τ (Oakes, 1989). A CRF greater than one corresponds to a positive association between T_1 and T_2. When $\theta^*(t_1, t_2)$, (2) allows for negative dependence between T_1 and T_2 but there is no frailty interpretation in this case. If T_1 and T_2 are independent, then $\theta^*(t_1, t_2) = 1$.

In shared frailty models for bivariate survival data the distribution of Z in (1) is identifiable through the CRF. To relate (2) to the distribution of Z consider the relationship (Anderson et al., 1992):

$$\theta^*(t_1, t_2) = \frac{\mathrm{Var}(Z|\, T_1 > t_1, T_2 > t_2)}{[\mathrm{E}(Z|\, T_1 > t_1, T_2 > t_2)]^2} + 1 \ , \tag{3}$$

where the first term on the right side of equation (3) is the square of the coefficient of variation of Z given $T_1 > t_1$ and $T_2 > t_2$. The representation (3) provides a readily interpretable measure of how the heterogeneity of the hazard functions of survivors, as represented by a frailty model, evolves over time. It is well established that the gamma frailty distribution is the only continuous distribution with constant $\theta^*(t_1, t_2)$ and that (3) decreases with time e.g. for the inverse Gaussian and increases with time e.g. for the compound Poisson frailties. However, more diverse shapes of the CRF are possible. For example, Paik et al. (1994) state that "*...no frailty models are known to yield...bathtub-shaped dependence function.*". Farrington et al. (2012) give evidence that bathtub-shaped cross-ratio functions can arise in the context of mixed distributions, which have an atom at zero and are continuous on the positive real line. They present an example with a bathtub-shaped profile that arises from a mixed distribution in which the continuous component is inverse Gaussian.

Normal distributions and Student-t distributions are not possible families of frailty distributions, as these have support $(-\infty, \infty)$. However, truncated and folded versions of normal and Student-t distributions may be adequate candidates for frailty distributions. In this paper we investigate the shape of the dependence structures that are induced by members of the class of truncated and folded normal frailty distributions.

The remainder of the paper is organized as follows. In Section 2, some results are presented that are useful for further analyses. We explore the shape of the CRF generated by truncated (folded) normal frailty distributions in Section 3 (Section 4). A discussion in Section 5 concludes. Computations for this manuscript were carried out using the R Software, version 3.2.1 (R Core Team, 2015). All computer code used is available upon request.

2. The rescaled cross-ratio function

In a shared frailty model such as (1), the frailty Z solely generates the association structure between T_1 and T_2. This means that an association measure should be free from the influence of

$$H_{0j}(t) = \int_0^t h_{0j}(u)\,\mathrm{d}u \ ,$$

where $H_{0j}(t)$ are the cumulative baseline hazards ($j = 1, 2$). Oakes (1989) showed that if the shared frailty model (1) holds, the CRF depends on (t_1, t_2)

only through some function $\theta(\nu)$ of the joint survivor function $\nu = S(t_1, t_2)$. This means that $\theta^*(t_1, t_2) = \theta(S(t_1, t_2)) = \theta(\nu)$. The function $\theta(\nu)$ determines the frailty distribution up to a scale factor (Oakes, 1989). Farrington et al. (2012) showed that

$$\theta^*(t_1, t_2) = \theta(\mu \cdot (H_{01}(t_1) + H_{02}(t_2))) \ ,$$

where μ denotes the frailty mean. Thus, the CRF depends on (t_1, t_2) only through $\mu \cdot (H_{01}(t_1) + H_{02}(t_2))$ and may be characterized independently of the cumulative baseline hazards by rescaling the time axis. Thus, we can set $s = \mu \cdot (H_{01}(t_1) + H_{02}(t_2))$ and define $\theta(s) = \theta^*(t_1, t_2)$. The rescaled CRF, $\theta(s)$, is a feature solely of the frailty Z. Suppose that Z has cumulative distribution function (cdf) $F(z)$, Laplace transform

$$\mathcal{L}(s) = \mathrm{E}\left\{\exp(-sZ)\right\} = \int_0^\infty \exp(-sz)\,\mathrm{d}F(z)$$

and cumulant-generating function $\mathcal{K}(s) = \ln\left\{\mathcal{L}(-s)\right\}$. The rescaled CRF can rewritten in terms of $\mathcal{K}(s)$ as follows (Aalen et al., 2008; Farrington et al., 2012):

$$\theta(s) = \frac{\mathcal{K}''(-s/\mu)}{\mathcal{K}'(-s/\mu)^2} + 1 = \frac{\mathcal{K}''(-(H_{01}(t_1) + H_{02}(t_2)))}{\mathcal{K}'(-(H_{01}(t_1) + H_{02}(t_2)))^2} + 1 \ , \tag{4}$$

where the prime denotes differentiation with respect to its argument. The expression (4) may ease the computational burden for calculating the CRF for shared frailty distributions. In Figure 1 profiles of the rescaled CRFs are displayed for various frailty distributions.

[Figure 1 about here.]

Figure 1 shows that the CRF can take many shapes. When bivariate time-to-event data are thought to arise from a shared frailty model, diagnostic plots based on the CRF may be used to suggest an appropriate frailty distribution or class of distributions (Viswanathan and Manatunga, 2001; Duchateau and Janssen, 2008).

3. Truncated normal frailty distributions

Suppose a continuous random variable Y has a standard normal distribution, that is, $Y \sim \mathcal{N}(0, 1)$. For $\xi \in \mathbb{R}$ and $\sigma > 0$, let $X = \xi + \sigma Y$. The two-parameter family of distributions associated with $X \sim \mathcal{N}(\xi, \sigma^2)$ is called the location-scale family associated with the given distribution of Y; ξ is the location parameter and σ the scale parameter. The resulting Laplace transform of X is

$$\mathrm{E}\left\{\exp(-sX)\right\} = \exp\left(\frac{\sigma^2 s^2}{2} - \xi s\right) \quad . \tag{5}$$

The two-parameter location-scale family of distributions with Laplace transform (5) is not a possible family of distributions for the frailty $Z \geq 0$, since their members have support on the whole real line. As a remedy, one may consider a one-sided truncated version of the pdf of X instead, that is, a conditional density that results from restricting the domain of $f_X(x) = \frac{1}{\sqrt{2\pi}\sigma}\exp\left(-\frac{(x-\xi)^2}{2\sigma^2}\right)$ for $-\infty < x < \infty$ to the interval $[0, \infty)$. Suppose that the frailty Z represents the truncated distribution of X over the support $[0, \infty)$. Then, the density of Z is given by

$$f_Z(z) = \frac{\sigma^{-1}\phi\left(\frac{z-\xi}{\sigma}\right)}{1 - \Phi\left(\frac{0-\xi}{\sigma}\right)} \quad , \quad 0 \leq z < \infty \quad , \tag{6}$$

where $\phi(\cdot)$ and $\Phi(\cdot)$ are the pdf and cdf of the standard normal variable, respectively. The mean and variance of Z are

$$\mu = \mathrm{E}(Z) = \xi + \sigma\lambda(\alpha)$$

and

$$\mathrm{Var}(Z) = \sigma^2[1 - \delta(\alpha)] \ ,$$

respectively, where $\alpha = -\xi/\sigma$, $\lambda(\alpha) = \phi(\alpha)/[1-\Phi(\alpha)]$ and $\delta(\alpha) = \lambda(\alpha)[\lambda(\alpha)-\alpha]$. The Laplace transform of Z is

$$\begin{aligned} \mathcal{L}(s) &= \int_0^\infty \exp(-sz) f_Z(z)\,\mathrm{d}z \qquad (7) \\ &= \exp\left(\frac{\sigma^2 s^2}{2} - \xi s\right) \frac{1 - \Phi\left(-\frac{\xi}{\sigma} + \sigma s\right)}{1 - \Phi(-\frac{\xi}{\sigma})} \end{aligned}$$

and the cumulant-generating function $\mathcal{K}(s) = \ln\left\{\mathcal{L}(-s)\right\}$ is

$$\begin{aligned} \mathcal{K}(s) &= \left(\frac{\sigma^2 s^2}{2} + \xi s\right) + \ln\left(1 - \Phi\left(-\frac{\xi}{\sigma} - \sigma s\right)\right) \qquad (8) \\ &\quad - \ln\left(1 - \Phi\left(-\frac{\xi}{\sigma}\right)\right) \quad . \end{aligned}$$

Hence,

$$\mathcal{K}(-s/\mu) = \left(\frac{\sigma^2(s/\mu)^2}{2} - \xi s/\mu\right) + \ln\left(1 - \Phi\left(-\frac{\xi}{\sigma} + \sigma s/\mu\right)\right) - c \ , \tag{9}$$

where c is a constant. In order to investigate the shape of the CRF that results from using truncated normal frailty distributions one has to obtain the expression on the right-hand side of equation (4), in other words, the first and second derivative of (9). For the one-sided truncated normal distribution, the derivatives $\mathcal{K}'(-s/\mu)$ and $\mathcal{K}''(-s/\mu)$ are specified by the equations (A.1)–(A.2) in the Appendix. In Figure 2 (i) four different pdfs of one-sided truncated normal frailty distributions with support $[0,\infty)$ are displayed.

[Figure 2 about here.]

Figure 2 (ii) shows the association patterns induced by the use of the one-sided truncated normal frailty distributions that are displayed in Figure 2 (i). As can be seen from Figure 2 (ii), for all distributions under investigation the scaled CRF, $\theta(s)$, increases as s increases. In fact, the CRFs are increasing towards positive asymptotes. The locations and slopes of the curves of the solid, dotted and dot-dashed curves are quite different, though. Note that for all one-sided truncated normal frailty distributions with $\xi = 0$ both the first derivative (A.1) and the second derivative (A.2) do not vary with respect to σ. Therefore, the solid and dashed lines coincide. The shape of the latter two trajectories is similar to the example from the Kummer family with increasing CRF shown in Figure 1 (ii).

4. Folded normal frailty distributions

If X is a random variable that follows a normal distribution with mean ξ and standard deviation σ, then $Z = |X|$ has a folded normal distribution with parameters ξ and σ. The density of Z is

$$f_Z(z) = \frac{1}{\sigma}\left[\phi\left(\frac{z-\xi}{\sigma}\right) + \phi\left(\frac{z+\xi}{\sigma}\right)\right] \quad , \quad z \in [0,\infty) \ . \tag{10}$$

The mean of Z is

$$\mu = \mathrm{E}(Z) = \xi[1 - 2\Phi(-\xi/\sigma)] + \sigma\sqrt{2/\pi}\exp\left(\frac{-\xi^2}{2\sigma^2}\right)$$

and the variance is

$$\mathrm{Var}(Z) = \xi^2 + \sigma^2 - \mu^2 \ .$$

Note that the truncated normal density is the positive part of the normal density, scaled up to have unit area, whereas the folded distribution is the sum of the positive part of the normal curve and its negative tail (as reflected around the vertical axis). If $\xi = 0$ in (10), the half-normal distribution is obtained, which coincides with a zero-mean normal distribution truncated from below at zero. For $\xi \neq 0$, however, the density (10) is different from the density (6).
The Laplace transform of Z is

$$\begin{aligned} \mathcal{L}(s) &= \exp\left(\frac{\sigma^2 s^2}{2} - \xi s\right)\left[1 - \Phi\left(-\frac{\xi}{\sigma} + \sigma s\right)\right] \\ &\quad + \exp\left(\frac{\sigma^2 s^2}{2} + \xi s\right)\left[1 - \Phi\left(\frac{\xi}{\sigma} + \sigma s\right)\right] \ . \end{aligned} \tag{11}$$

The cumulant-generating function of Z is

$$\begin{aligned} \mathcal{K}(s) &= \left(\frac{\sigma^2 s^2}{2} + \xi s\right) + \ln\left\{1 - \Phi\left(-\frac{\xi}{\sigma} - \sigma s\right)\right. \\ &\quad \left. + \exp(-2\xi s)\left[1 - \Phi\left(\frac{\xi}{\sigma} - \sigma s\right)\right]\right\} \ . \end{aligned} \tag{12}$$

Hence,

$$\begin{aligned} \mathcal{K}(-s/\mu) &= \left(\frac{\sigma^2 (s/\mu)^2}{2} - \xi s/\mu\right) + \ln\left\{1 - \Phi\left(-\frac{\xi}{\sigma} + \sigma s/\mu\right)\right. \\ &\quad \left. + \exp(2\xi s/\mu)\left[1 - \Phi\left(\frac{\xi}{\sigma} + \sigma s/\mu\right)\right]\right\} \ . \end{aligned} \tag{13}$$

The derivatives $\mathcal{K}'(-s/\mu)$ and $\mathcal{K}''(-s/\mu)$, which are required to compute the CRF in (4), are given in the equations (A.3)–(A.4) in the Appendix. In Figure 3 (i) four different pdfs of folded normal frailty distributions are displayed.

[Figure 3 about here.]

Figure 3 (ii) shows the association patterns induced by the use of folded normal frailty distributions that are displayed in Figure 3 (i). The solid curve represents the half-normal distribution (with frailty mean $\mu = 1$) and coincides with the solid and dashed curves in Figure 2 (ii), both of which representing one-sided truncated normal frailty distributions with $\xi = 0$ (but different scale parameter σ). At low s values there are slight differences between the solid and dotted lines; apart from this feature both curves are virtually identical and both curves do intersect with the dashed curve. For small values of σ the association pattern becomes virtually flat. The dot-dashed line virtually corresponds to the case of independence between the two survival variables and $\theta(s) = 1$.

5. Discussion

This paper has focused on Clayton's cross-ratio function for assessing time-varying dependence in models for bivariate survival data. We have considered models in which the dependence between the two failure times of interest is generated by a shared frailty that acts multiplicatively on the hazard. Shared frailty models have a wide applicability in a multivariate context, for example to model related individuals (e.g. twins), to model related components (e.g. right and left eye) in individuals, to model the case of recurrent events (e.g. epileptic seizures) or to model event times that arise from experiments, where a single individual goes through multiple treatments and for each treatment the time to some event is recorded (Hougaard, 2014). We have explored the shape of the CRF for the families of truncated and folded normal frailty distributions. As one can see from this paper, the shape of the CRF can take diverse profiles. For appropriate bivariate survival data at hand, plots of the estimated CRF, suitably rescaled, can serve as an exploratory tool for suggesting frailty distributions with a shape of the CRF that matches the observed profile.

The truncated normal and the folded normal can be viewed as the limit of the truncated and folded Student-t distribution, respectively, as the degrees of freedom go to infinity. One may want to study the shape of the CRF for truncated and folded Student-t distributions as well. In some settings it is more convenient to write the model (1) as

$$h_j(t, U) = \exp(U) \cdot h_{0j}(t) \ , \quad j = 1, 2 \ ,$$

obtained by setting $Z = \exp(U)$. In this model, $U = \ln(Z)$ is a random effect in the linear component of the proportional hazards model. Note that whereas $Z \geq 0$, U can take any value, positive or negative, and $U = 0$ corresponds to the case when $Z = 1$ and there is no frailty. For example, if $U \sim \mathcal{N}(0, \sigma_u^2)$, then Z has a log-normal distribution. Sahu and Dey (2004) assume that the distribution of $Z = \exp(U)$ is a member of the general class of log-skew-t distributions obtained in Azzalini and Kotz (2003) and discussed in Azzalini and Capitanio (2014). The class of log-skew-t distributions includes the log-skew normal distribution for which the dependence structure via the CRF has been studied by Callegaro and Iacobelli (2012). However, for the proposed class of log-skew-t frailty distributions, Sahu and Dey (2004) do not explore the dependence structure via the (local) CRF but consider the correlation between log-survival times as a (global) measure of dependence instead. Investigating the shape of the CRF arising from using various log-skew-t frailty distributions is one possible avenue for further research.

Frailty modelling is fraught with a lack of identifiability. For example, the temporal pattern in the association could be due to a time-varying frailty or to selection effects stemming from a time-invariant frailty, and there is no way of distinguishing between them. Note that with time-varying frailties, it is not possible to rescale the time axis to remove the dependence on the baseline hazards (Farrington et al., 2012). Nevertheless, the CRF in (2) can still be used. Furthermore, in our paper, we have assumed in (4) that the frailty has a finite but unspecified mean. In practical applications, it is advantageous to work with frailties of unit mean to separate the frailty model from the model for the baseline hazards.

Finally, the assumption of a shared frailty between two time variables is probably somewhat simplistic. In some situations, it is likely that that some heterogeneity is shared, but supplemented by heterogeneity that is specific to each variable. In such situations, correlated frailty models may be used (Wienke, 2011). Correlated frailty models add flexibility, but also make the model set-up more complicated and show lack of identifiability of the unshared components of the frailties. However, one should be aware that the heterogeneity that is captured by a shared frailty is, in some circumstances, most likely only part of the heterogeneity.

Acknowledgement

The author gratefully acknowledges David Ellenberger for proofreading the manuscript.

References

Aalen, O. O., Borgan, Ø., Gjessing, H. K., 2008. Survival and Event History Analysis: A Process Point of View. Springer: New York.

Anderson, J. E., Louis, T. A., Holm, N. V., Harvald, B., 1992. Time-dependent association measures for bivariate survival distributions. Journal of the American Statistical Association 87, 641–650.

Azzalini, A., Capitanio, A., 2014. The Skew-Normal and Related Families. Cambridge University Press: Cambridge.

Azzalini, A., Kotz, S., 2003. Log-skew-normal and log-skew-t distributions as models for family income data. Journal of Income Distribution 11, 12–20.

Callegaro, A., Iacobelli, S., 2012. The cox shared frailty model with log-skew normal frailties. Statistical Modelling 12, 399–418.

Clayton, D. G., 1978. A model for association in bivariate life tables and its application in epidemiological studies of family tendency in chronic disease incidence. Biometrika 65, 141–151.

Clayton, D. G., Cuzick, J., 1985. Multivariate generalizations of the proportional hazards model. Journal of the Royal Statistical Society, Series A 148, 82–117.

Duchateau, L., Janssen, P., 2008. The Frailty Model. Springer: New York.

Farrington, C. P., Unkel, S., Anaya-Izquierdo, K., 2012. The relative frailty variance and shared frailty models. Journal of the Royal Statistical Society Series B 74, 673–696.

Hougaard, P., 2000. Analysis of Multivariate Survival Data. Springer: New York.

Hougaard, P., 2014. Frailty models. In: Klein, J. P., van Houwelingen, H. C., Ibrahim, J. G., Scheike, T. H. (Eds.), Handbook of Survival Analysis. Chapman and Hall: CRC, pp. 457–474.

Oakes, D., 1989. Bivariate survival models induced by frailities. Journal of the American Statistical Association 84, 487–493.

Paik, M. C., Tsai, W.-Y., Ottman, R., 1994. Multivariate survival analysis using piecewise gamma frailty. Biometrics 50, 975–988.

R Core Team, 2015. R: A Language and Environment for Statistical Computing. R Foundation for Statistical Computing, Vienna, Austria. URL https://www.R-project.org

Sahu, S. K., Dey, D. K., 2004. On a Bayesian multivariate survival model with a skewed frailty. In: Genton, M. G. (Ed.), Skew-Elliptical Distributions and Their Applications: A Journey Beyond Normality. CRC/Chapman & Hall: Boca Raton, FL, pp. 321–338.

Viswanathan, B., Manatunga, A. K., 2001. Diagnostic plots for assessing the frailty distribution in multivariate survival data. Lifetime Data Analysis 7, 143–155.

Wienke, A., 2011. Frailty Models in Survival Analysis. Chapman & Hall/CRC Press: Boca Raton, FL.

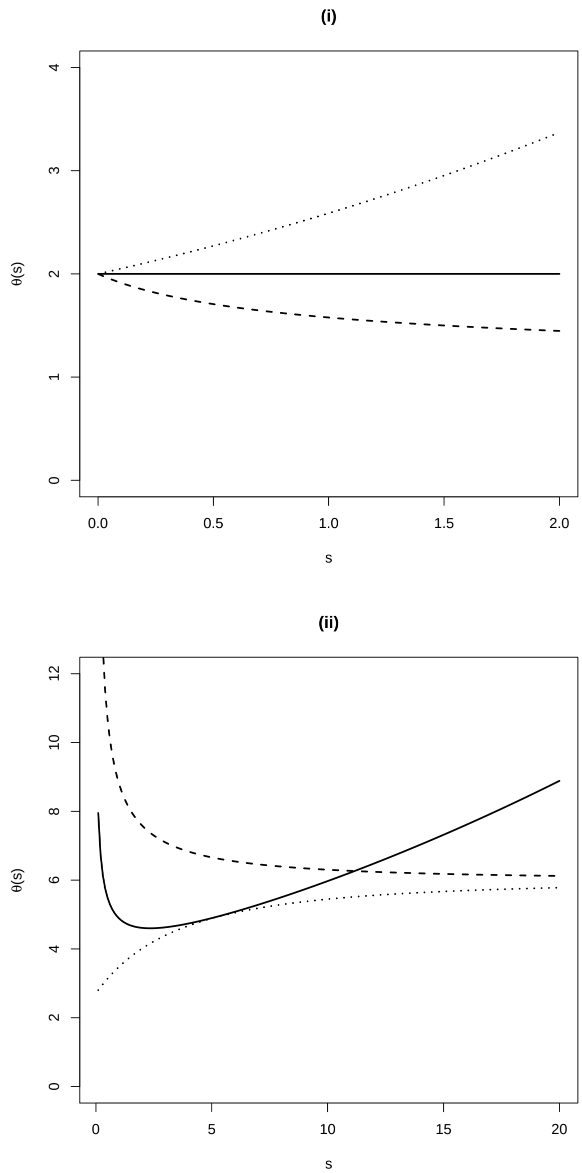

Figure 1: Scaled cross-ratio functions generated by shared frailty distributions: (i) gamma (solid line), inverse Gaussian (dashed line) and compound Poisson model (dotted line); (ii) mixed frailty model with atom $P(Z = 0) = 0.5$ and inverse Gaussian continuous component (solid line), frailties from the Kummer family (Farrington et al., 2012) with decreasing CRF (dashed line) and increasing CRF (dotted line).

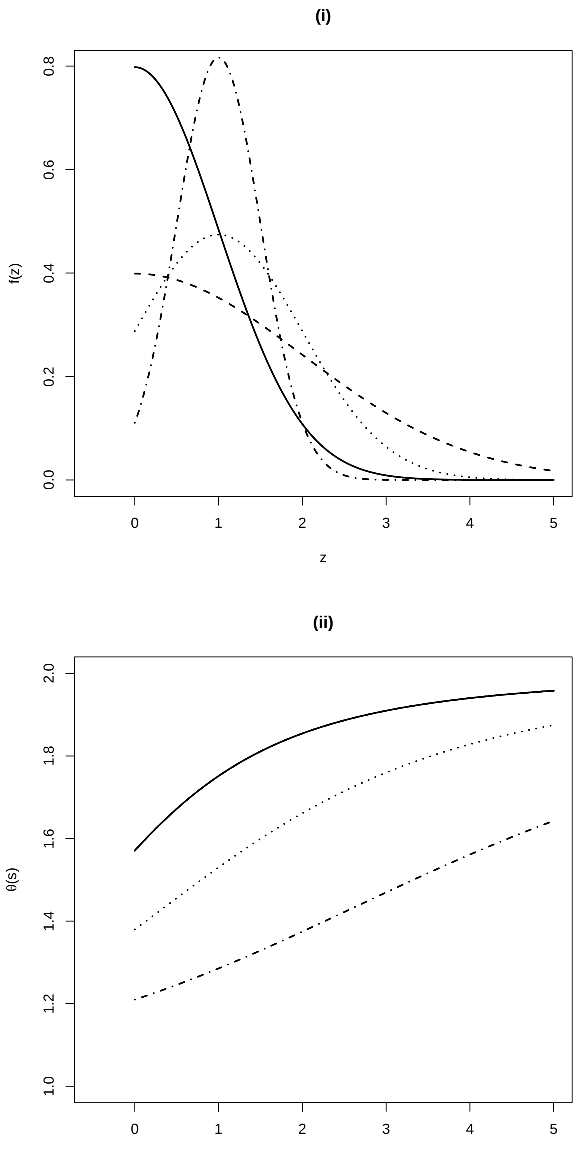

Figure 2: (i) density for the truncated normal distribution with support $[0, \infty)$ for different sets of parameters: $\xi = 0$, $\sigma = 1$ (solid line), $\xi = 0$, $\sigma = 2$ (dashed line), $\xi = 1$, $\sigma = 1$ (dotted line), $\xi = 1$, $\sigma = 0.5$ (dot-dashed line); (ii) scaled CRFs induced by one-sided truncated normal frailty distributions displayed in (i).

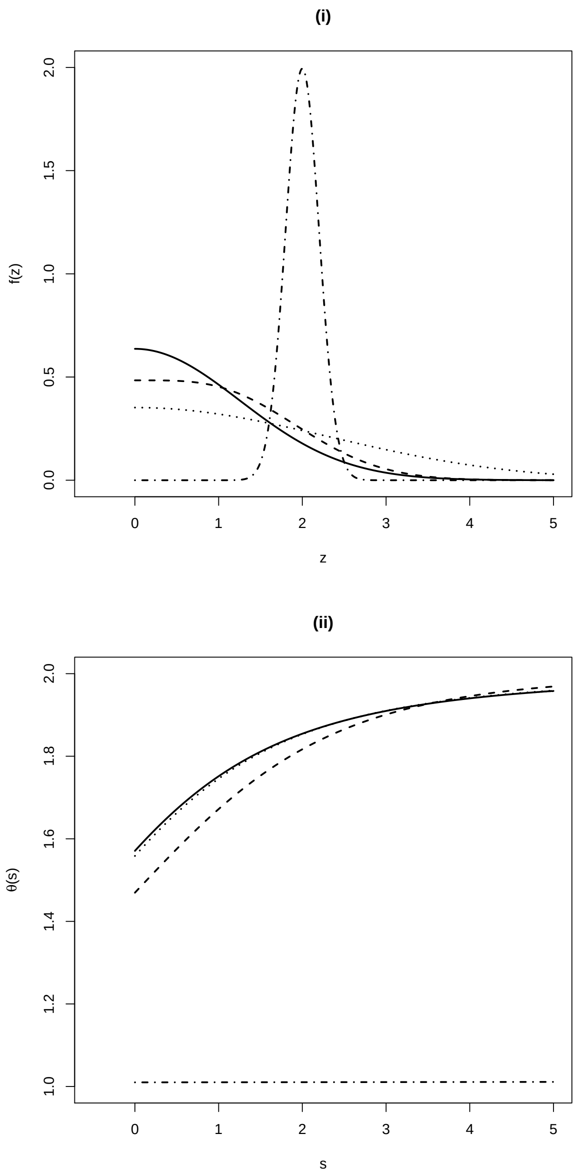

Figure 3: (i) density for the folded normal distribution for different sets of parameters: $\xi = 0$, $\sigma = \sqrt{\pi/2}$ (solid line), $\xi = 1$, $\sigma = 1$ (dashed line), $\xi = 1$, $\sigma = 2$ (dotted line), $\xi = 2$, $\sigma = 0.2$ (dot-dashed line); (ii) scaled CRFs induced by folded normal frailty distributions displayed in (i).

Appendix

One-sided truncated normal distribution

$$\mathcal{K}'(-s/\mu) = \frac{\sigma^2 s}{\mu^2} - \frac{\xi}{\mu} - \frac{\sigma\phi\left(\frac{\sigma s}{\mu} - \frac{\xi}{\sigma}\right)}{\mu\left(1 - \Phi\left(\frac{\sigma s}{\mu} - \frac{\xi}{\sigma}\right)\right)} \tag{A.1}$$

$$\mathcal{K}''(-s/\mu) = \frac{\sigma^2}{\mu^2} - \frac{\sigma^2\phi\left(\frac{\sigma s}{\mu} - \frac{\xi}{\sigma}\right)^2}{\mu^2\left(1 - \Phi\left(\frac{\sigma s}{\mu} - \frac{\xi}{\sigma}\right)\right)^2} - \frac{\sigma^2\phi'\left(\frac{\sigma s}{\mu} - \frac{\xi}{\sigma}\right)}{\mu^2\left(1 - \Phi\left(\frac{\sigma s}{\mu} - \frac{\xi}{\sigma}\right)\right)} \tag{A.2}$$

Folded normal distribution

$$\mathcal{K}'(-s/\mu) = \frac{2\xi\exp(2\xi s/\mu)\left(1 - \Phi\left(\frac{\sigma s}{\mu} + \frac{\xi}{\sigma}\right)\right) - \sigma\phi\left(\frac{\sigma s}{\mu} - \frac{\xi}{\sigma}\right) - \sigma\exp(2\xi s/\mu)\phi\left(\frac{\sigma s}{\mu} + \frac{\xi}{\sigma}\right)}{\mu\left\{1 - \Phi\left(\frac{\sigma s}{\mu} - \frac{\xi}{\sigma}\right) + \exp(2\xi s/\mu)\left[1 - \Phi\left(\frac{\sigma s}{\mu} + \frac{\xi}{\sigma}\right)\right]\right\}} + \frac{\sigma^2 s}{\mu^2} - \frac{\xi}{\mu} \tag{A.3}$$

$$\begin{aligned}\mathcal{K}''(-s/\mu) = \frac{1}{\mu^2}\Bigg\{&\frac{4\xi^2\exp(2\xi s/\mu)\left(1 - \Phi\left(\frac{\sigma s}{\mu} + \frac{\xi}{\sigma}\right)\right) - \sigma^2\phi'\left(\frac{\sigma s}{\mu} - \frac{\xi}{\sigma}\right) - \sigma^2\exp(2\xi s/\mu)\phi'\left(\frac{\sigma s}{\mu} + \frac{\xi}{\sigma}\right) - 4\xi\sigma\exp(2\xi s/\mu)\phi\left(\frac{\sigma s}{\mu} + \frac{\xi}{\sigma}\right)}{1 - \Phi\left(\frac{\sigma s}{\mu} - \frac{\xi}{\sigma}\right) + \exp(2\xi s/\mu)\left(1 - \Phi\left(\frac{\sigma s}{\mu} + \frac{\xi}{\sigma}\right)\right)} \\ &- \frac{\left(2\xi\exp(2\xi s/\mu)\left(1 - \Phi\left(\frac{\sigma s}{\mu} + \frac{\xi}{\sigma}\right)\right) - \sigma\phi\left(\frac{\sigma s}{\mu} - \frac{\xi}{\sigma}\right) - \sigma\exp(2\xi s/\mu)\phi\left(\frac{\sigma s}{\mu} + \frac{\xi}{\sigma}\right)\right)^2}{\left(1 - \Phi\left(\frac{\sigma s}{\mu} - \frac{\xi}{\sigma}\right) + \exp(2\xi s/\mu)\left(1 - \Phi\left(\frac{\sigma s}{\mu} + \frac{\xi}{\sigma}\right)\right)\right)^2} + \sigma^2\Bigg\}\end{aligned} \tag{A.4}$$